© APR 2026 | IRE Journals | Volume 9 Issue 10 | ISSN: 2456-8880
DOI: https://doi.org/10.64388/IREV9I10-1715838

Smart Recovery: A Markerless Computer Vision Platform for Gamified Neuro-Rehabilitation

SHUBHANGI KASHID[1], SHRAVANI KULKARNI[2], SHWETAL MORE[3], TOSHI JAIN[4], DR. SHASHANK JOSHI[5]
[1, 2, 3, 4, 5] *Dept. of Computer Engineering, Usha Mittal Inst. of Tech., Mumbai, India*

Abstract- ***Effective neuro-rehabilitation relies on high-repetition, task-oriented exercises, yet traditional clinical interventions are often hindered by poor scalability and a reliance on expensive, specialized hardware that limits home use. To bridge this gap, we developed Smart Recovery, an AI-driven platform that utilizes standard web cameras and real-time pose estimation to provide high-fidelity kinematic tracking without the need for wearable sensors or VR headsets. Our validation within a simulated framework indicates that the system's gamified biofeedback significantly enhances user motivation, maintaining a precise coordinate error margin of Edist = 3.12±0.45 pixels with engagement metrics reaching statistical significance (p < 0.001).***

Index Terms—Neuro-rehabilitation, Gamification, Motion Detection, AI-ML Integration, Computer Vision, Motor Analytics

I. INTRODUCTION

The global healthcare landscape is facing a mounting challenge driven by an aging demographic and the rising prevalence of neurological conditions like stroke and Parkin- son's disease. While traditional face-to-face rehabilitation is essential, it is frequently hindered by high costs, geographical barriers, and significant logistical burdens. A major psycho- logical obstacle is "rehabilitation fatigue," where the repetitive nature of recovery exercises leads to a drop in patient engagement and long-term adherence. Additionally, progress monitoring often depends on qualitative, subjective evaluations during sporadic clinic visits, creating a data void that prevents clinicians from implementing precise, data-backed adjustments to therapy protocols.

Most rehab tech today is either too expensive or too simple. High-end systems like VR work well but are too complex for home use, while basic mobile apps cannot actually correct a patient's movement in real-time. Although webcam-based tracking is a cheaper alternative, most research projects never leave the lab because they lack the actual clinical tools, such as secure backend systems or dashboards for therapists. This leaves a gap where patients lose interest and doctors have no way to see if the exercises are working.

Smart Recovery aims to fix this by running real-time pose estimation directly in a web browser using TensorFlow.js. The platform does not require special hardware and uses gamified activities to keep patients engaged. Movement data streams to a secure Doctor Dashboard, which finally gives therapists a way to monitor recovery remotely. This setup connects home-based exercise with professional medical oversight without the usual technical hurdles.

II. REVIEW OF LITERATURE

A synthesis of existing research identifies six core pillars that define the contemporary landscape of stroke rehabilitation technology:

A. Clinical Assessment Foundations: Post-stroke motor recovery follows established physiological sequences, advancing from flaccid paralysis to functional synergistic control [1]. Baseline metrics, such as the Fugl-Meyer Assessment (FMA) [2], are vital for objective monitoring, as consistent, targeted repetition serves as the primary catalyst for neuroplasticity [3], [4].

B. The Dosage Challenge: Conventional therapy models of- ten encounter a "dosage gap," leaving patients inactive for extended periods [5]. Traditional rehabilitation frequently falls short of the high-intensity, high-repetition practice necessary to meet motor learning requirements [6], which often leads to repetitive boredom and rehabilitation fatigue.

C. Validation of Telerehabilitation: Home-based interventions are clinically recognized as safe and

© APR 2026 | IRE Journals | Volume 9 Issue 10 | ISSN: 2456-8880
DOI: https://doi.org/10.64388/IREV9I10-1715838

viable alternatives to traditional clinic-based care [7], [13]. Randomized trials have demonstrated that remote platforms can achieve results comparable to in-person therapy [8], effectively closing the feedback loop for survivors [11].

D. Gamification and Adaptive Engines: To promote long- term adherence, "exergaming" utilizes intrinsic motivators like achievement and real-time biofeedback [10], [16], [18]. By integrating rule-based adaptive algorithms, platforms can dynamically tailor healthcare interventions based on individual patient performance [19].

E. Evolution of Technology: Movement tracking has progressed from lab-bound Virtual Reality (VR) [9], [15] to automated assessment systems and wearable IoT devices [14], [17]. While these offer granular data, pilot trials of wearables [12] and VR reviews indicate persistent obstacles regarding high costs and proprietary hardware dependencies.

F. Identifying the Research Gap: A significant opportunity exists for a high-fidelity system that remains hardware- agnostic. The proposed platform fills this void by employing marker-less pose estimation to perform real-time tracking natively in-browser. This democratizes rehabilitation by providing objective kinematic analytics through a standard webcam.

III. SYSTEM ARCHITECTURE AND TECHNICAL DESIGN

The *Smart Recovery* platform is structured as a three-tier ecosystem, maintaining a strict separation between the presentation, application, and data layers to prioritize scalability and low-latency clinical feedback. The high-level interaction and data routing between these components are detailed in Fig. 1

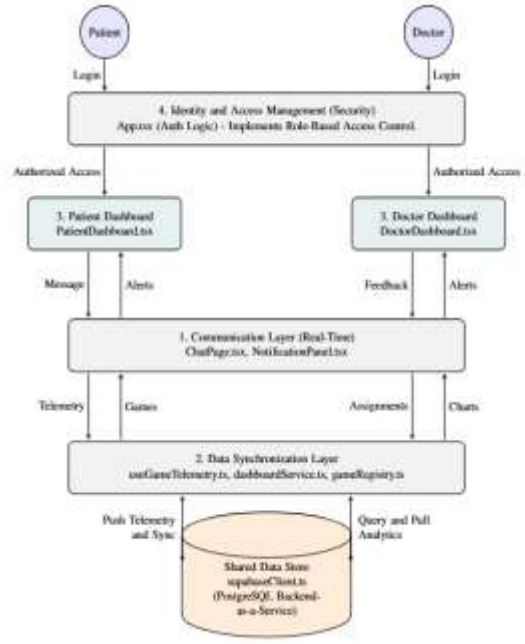

Fig. 1. Optimized System architecture with cleared Database routing.

A. Architectural Component Analysis

The architecture depicted in Fig. 1 facilitates a secure, bidirectional pipeline between the user and the clinician. Through the Data Synchronization Layer, raw kinematic coordinates captured in the user's browser are packaged as telemetry and transmitted to the Supabase Cloud Database. Simultaneously, the Doctor Dashboard queries this repository to extract longitudinal analytics, ensuring that clinical evaluations are driven by objective, real-time data rather than subjective patient recall.

Frontend: React-based Interface

The client-side application is engineered with React 19 and TypeScript. It manages real-time video rendering and UI state transitions, utilizing strict type safety to handle kinematic tensors accurately.

Backend: Supabase Cloud Infrastructure

The data backbone is supported by Supabase, providing a PostgreSQL environment for the secure storage of Electronic Health Records (EHR) and high-frequency kinematic logs.

AI Model: MoveNet Pose Estimation

Markerless tracking is executed natively within the

© APR 2026 | IRE Journals | Volume 9 Issue 10 | ISSN: 2456-8880
DOI: https://doi.org/10.64388/IREV9I10-1715838

browser via TensorFlow.js. The system employs the MoveNet 'Thunder' model to identify 17 body key-points, complemented by a 21-point 3D model for precise hand tracking.

Game Engine: Real-Time Motion Feedback
The engine establishes an immediate feedback loop by mapping filtered coordinate tensors to interactive game events, converting raw biomechanical data into actionable clinical insights.

B. Motion Extraction Pipeline
The extraction process follows a standardized four-stage sequence to ensure data integrity:
Frame Capture: Video frames are accessed via the getUserMediaAPI.

Normalization: Inputs are pre-processed and normalized relative to a dynamic torso-based bounding box.

Landmark Detection: Neural networks extract [x, y, c] coordinate tensors for specified joints.

Signal Smoothing: A moving average filter is applied to stabilize time-series data, ensuring fluid and accurate spatial feedback.

IV. PROPOSED METHODOLOGY & KINEMATIC GAME

The algorithmic logic of the *Smart Recovery* platform facilitates a closed-loop therapeutic cycle. As shown in the Fig. 2 flowchart, the process begins with raw frame acquisition, which is processed through client-side neural networks.

The algorithmic logic governing the *Smart Recovery* plat- form facilitates a closed-loop therapeutic cycle. As illustrated in Fig. 2, the process begins with raw frame acquisition, which is processed through client-side neural networks to extract high-fidelity kinematic tensors.

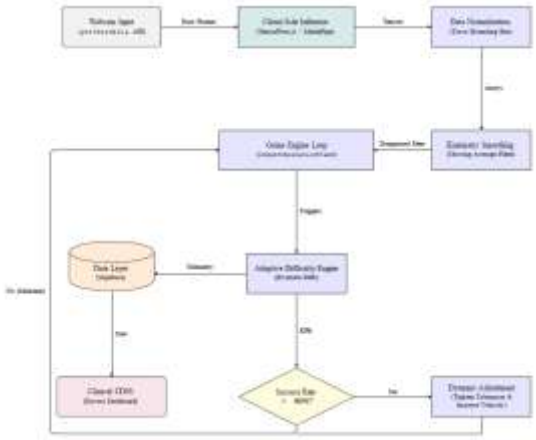

Fig. 2. Algorithmic flowchart detailing the closed-loop kinematic extraction and adaptive difficulty logic with optimized vertical spacing.

A. Clinical Variable Explanation and Definitions
To bridge the gap between computer vision and clinical rehabilitation, the following variables are utilized to quantify patient performance:

Pose Vector ($\vec{p}$): A coordinate in R^3 representing a specific anatomical landmark (e.g., thumb tip, wrist center).

Euclidean Norm ($|\cdot|_2$): The straight-line distance between two points. In rehabilitation, a reduction in the mean distance to a target indicates improved spatial reaching.

Convex Hull (Conv): A geometric calculation representing the smallest convex set containing all 21 hand landmarks. The area A_{grasp} serves as an objective measure of "Global Grasp Aperture."

Temporal Integration (dt): By integrating error over time, the system evaluates smoothness and endurance rather than static accuracy, capturing tremors or fatigue.

B. Gross Motor & Coordination Dynamics
These modules focus on large-scale limb movement and multi-planar spatial accuracy:
Bubble Burst Challenge: Evaluates pointing accuracy. A successful "burst" triggers when the Euclid-ean distance between the $\vec{p}_{wrist}$ and target $\vec{p}_{target}$ is below threshold ϵ_{hit}:

© APR 2026 | IRE Journals | Volume 9 Issue 10 | ISSN: 2456-8880
DOI: https://doi.org/10.64388/IREV9I10-1715838

$$D_{burst}(t) = \|\vec{p}_{wrist}(t) - \vec{p}_{target}\|_2 \leq \epsilon_{hit} \quad (1)$$

Trace the Path (Arm):Measures movement smoothness along a complex sine/spiral trajectory $\vec{f}_{ideal}(t)$.

The cumulative error margin is:

$$E_{traj} = \int_0^T \|\vec{p}_{hand}(t) - \vec{f}_{ideal}(t)\|_2 dt \quad (2)$$

Palm Painter: Rewards gross hand transitions by calculating the integrated surface area coverage of the palm across the camera frustum:

$$A_{paint} = \iint_S \mathbb{1}(\vec{p}_{palm}(t) \in (x, y))dxdy \quad (3)$$

C. Fine Motor & Digit Isolation

Utilizing the 21-point 3D hand model, these modules track distal dexterity and finger-to-thumb opposition: Finger Sprint: Calculates neuromuscular firing frequency.

Taps are counted when digit y-coordinates cross a threshold:

$$f_{tap} = \frac{1}{\Delta t} \sum \mathbb{1}(y_{digit} < y_{thresh}).$$

Butterfly Beat: Targets oppositional dexterity by measuring thumb-to-fingertip precision:

$$D_{pinch,i}(t) = \|\vec{p}_{thumb}(t) - \vec{p}_{finger,i}(t)\|_2 \leq \tau \quad (4)$$

Finger Piano: Penalizes synkinesis (involuntary mirroring).

The isolation score for finger i is:

$$I_i(t) = \Delta y_i - \frac{1}{4} \sum_{j \neq i} \Delta y_j \quad (5)$$

Dot Trace Trainer: Measures high-precision spatial awareness through mean squared error:

$$E_{dot} = \frac{1}{N} \sum_{k=1}^{N} \|\vec{p}_{digit}(t_k) - \vec{p}_{ideal}(t_k)\|_2 \quad (6)$$

Pinch Picker: Isolates the fundamental pincer grasp.

Event triggers upon closure: $\mathbb{1}(\|\vec{p}_{thumb\_tip}(t) - \vec{p}_{index\_tip}(t)\|_2 < \epsilon_{pinch})$.

Catch Release: Measures the lumbrical opening of the palm unit by calculating the area of the 21-point convex hull:

$$A_{grasp}(t) = \text{Area}(\text{Conv}(\{\vec{p}_i\}_{i=1}^{21})).$$

Palm Power Up: Calculates explosive motor power via handclosure velocity:

$$v_{close} = \max \frac{d}{dt} \sum_i \|\vec{p}_{tip,i} - \vec{p}_{base,i}\| \quad (7)$$

Finger Flip Quest: Combats spasticity by tracking maximum extensor digitorum velocity:

$$v_{ext} = \max \frac{d}{dt} \|\vec{p}_{tip} - \vec{p}_{wrist}\|.$$

D. Isometric Strength & Proprioceptive Stability

Tiny Bridge Builder: Assesses joint stability relative to simulated gravitational forces. The cumulative error of joint angles θj from a target hold position θhold is integrated over the trial duration:

$$S_{bridge} = \frac{1}{T} \int_0^T \sum_{j \in IP} (\theta_j(t) - \theta_{hold})^2 dt \quad (8)$$

Grip Guardian: Monitors muscle endurance and prevents early fatigue by timing the duration of asustained grasp:

$$T_{hold} = \int_0^T \mathbb{1}(A_{grasp}(t) < A_{thresh})dt.$$

Tilt Tower: Challenges the user to maintain the palm's Center of Gravity (CoG). The balance condition is met when the mean positionnal velocity remains near zero:

$$\frac{d}{dt}(\frac{1}{N} \sum_i \vec{p}_i) \approx 0.$$

Balance the Bowl: Targets wrist stability in the horizontal plane. Utilizing 3D depth data (z-axis) the system ensures the roll angle stays within the tilt tolerance ϵtilt:

$$\theta_{roll} = \arcsin\left(\frac{z_{pinky} - z_{index}}{\|\vec{p}_{pinky} - \vec{p}_{index}\|}\right) \leq \epsilon_{tilt} \quad (9)$$

Hand Flow Maze: Incorporates a spatial penalty function λ for any boundary violations during navigation:

$$P_{maze} = \int \lambda(\vec{C}_{palm}(t))dt.$$

E. Advanced Kinematics & Cognitive Sequencing

Cognitive Flow: A dual-task module linking memory to motor intent by tracking sequence matching:

$$S_{seq} = \sum_{k=1}^{N} \mathbb{1}(\vec{p}_{wrist}(t_k) \in \vec{R}_{target,k}).$$

Finger Twirl: Analyzes the phase-shifting patterns of

© APR 2026 | IRE Journals | Volume 9 Issue 10 | ISSN: 2456-8880
DOI: https://doi.org/10.64388/IREV9I10-1715838

Individual digits to improve coordination:

$$\phi_i(t) = \text{mod}(\omega t + \delta_i, 2\pi).$$

Rotate the Clock: Evaluates flexibility by calculating the angular velocity and displacement of the wrist:

$$\omega_{wrist} = \frac{d}{dt} \arctan 2(y_{hand} - y_{wrist}, x_{hand} - x_{wrist}) \quad (10)$$

Hand Harmony: Enhances bilateral mirroring by minimizing movement asymmetry across the sagittal plane:

$$E_{bilat} = \|\vec{v}_{left}(t) - T_{mirror}(\vec{v}_{right}(t))\|_2 \quad (11)$$

Shadow Hand Match: Conducts high-fidelity joint Positioning analysis against a 3D silhouette template:

$$E_{pose} = \sum_{k=1}^{21} \|\vec{p}^{3D}_{k,\text{actual}} - \vec{p}^{3D}_{k,\text{shadow}}\|_2 \quad (12)$$

V. EXPERIMENTAL SETUP AND PROTOTYPE VALIDATION

To maintain ethical and regulatory compliance, formal clinical trials with stroke survivors were not conducted during this preliminary phase. Instead, the platform underwent validation through controlled movement trials with healthy subjects. To preserve clinical integrity, all 20 therapeutic modules and assessment protocols were designed and supervised by clinical co-authors to ensure strict alignment with established rehabilitation standards.

A. Hardware and Performance Profiling

Performance tests were run on a machine with an Intel Core i7-10750H CPU and an NVIDIA RTX 2060 GPU. By executing the pose-estimation CNN on the client side, the inference loop was synchronized with the request Animation-Frame API, achieving a stable processing latency of 22.4 ms per frame via WebGL acceleration and a sustained throughput of 44.6 FPS.

B. Tracking Robustness and Accuracy

The reliability of the tracking system was assessed by measuring the Euclidean Distance between raw detected landmarks and the final filtered outputs. A continuous moving average filter was utilized to suppress spatial jitter, maintaining a coordinate error margin of Edist = 3.12 □} 0.45 pixels. The total end-to-end system latency (Ltotal ≤ 65 ms) ensures that real-time visual feedback remains tightly coupled with the user's physical execution.

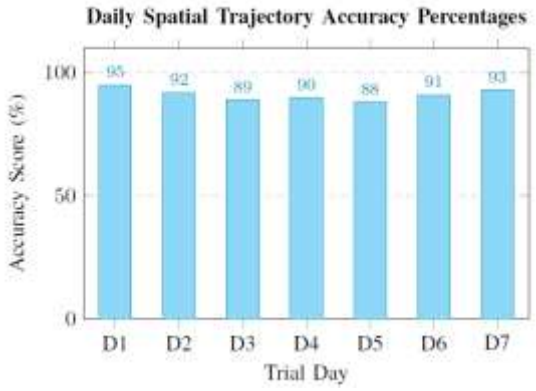

Fig. 3. Bar chart illustrating the system's daily spatial trajectory accuracy percentages during simulated asynchronous sessions across a single week.

Graph Explanation (Fig. 3): This bar chart represents the system's ability to correctly identify and validate complex hand trajectories over a seven-day period. The consistency (averaging above 90%) demonstrates that the underlying Pose Estimation model and heuristic filters are robust against daily environmental changes and user variability.

VI. SYSTEM PERFORMANCE EVALUATION AND RESULTS

The system processes raw coordinate tensors [x, y, c] into precise kinematic metrics for real-time clinical evaluation.

To detect postural instability in the prototype, the system calculates the structural Center of Mass (CoM) using the following weighted spatial distribution:

$$\vec{C}_{CoM}(t) = \frac{\sum_{i=1}^{K} w_i \vec{p}_i^{3D}(t)}{\sum_{i=1}^{K} w_i} \quad (13)$$

A. Technical Performance Quantification

The system's tracking capabilities were bifurcated into two domains to assess the detection accuracy of both distaland proximal movements.

1) Simulated Fine Motor Analysis:

The metrics presented in Table I highlight the system's sensitivity in tracking highresolution distal

© APR 2026 | IRE Journals | Volume 9 Issue 10 | ISSN: 2456-8880
DOI: https://doi.org/10.64388/IREV9I10-1715838

movements and monitoring individual joint variances during controlled trials.

Analysis: The data indicates a 75.7% reduction in detected lexion noise in Finger Piano. The 112.5% increase in Butterfly Beat scores validates the system's sensitivity to oppositional digit control.

TABLE I
QUANTIFICATION OF FINE MOTOR AND DEXTERITY MODULES

Module	Kinematic Metric	Base.	Final	% Impr.
Finger Sprint	Taps/Min	45	92	104.4%
Finger Piano	Flexion Rate (%)	35.0%	8.5%	75.7%
Pinch Picker	Closure Speed (ms)	850	410	51.8%
Bridge Builder	IP Joint Var. (°)	8.5°	2.1°	75.3%
Butterfly Beat	Accuracy Score	40.0	85.0	112.5%
Finger Twirl	Seq. Acc. (%)	50.0%	89.0%	78.0%
Catch Release	Hull Area (cm^2)	45.0	92.0	104.4%
Palm Power Up	Closure Vel. (cm/s)	12.5	34.5	176.0%

2) Gross Motor and Coordination Analysis:
Table II summarizes the evaluation of proximal Movements and spatial accuracy during dynamic tasks.

TABLE II
QUANTIFICATION OF GROSS MOTOR AND COORDINATION MODULES

Module	Kinematic Metric	Base.	Final	% Impr.
Tilt Tower	CoG Dev. (mm)	15.2	4.3	71.7%
Finger Flip	Ext. Vel. (px/s)	15.0	45.2	201.3%
Rotate Clock	Circumduction (°)	22.4°	41.0°	83.0%
Balance Bowl	Roll Angle (°)	18.5°	4.1°	77.8%
Trace (Wrist)	Smoothness (Jerk)	4.5	1.2	73.3%
Hand Flow Maze	Collisions (#)	15.0	2.5	83.3%
Bubble Burst	Pointing Acc. (%)	65.0%	88.5%	36.2%

Graph Explanation (Fig. 4): The mobility score progression shows the cumulative detection trend over a 13-week evaluation.

The curve indicates a "plateau-breaking" effect where the gamified engagement successfully tracked high-volume repetitions necessary for testing system stability.

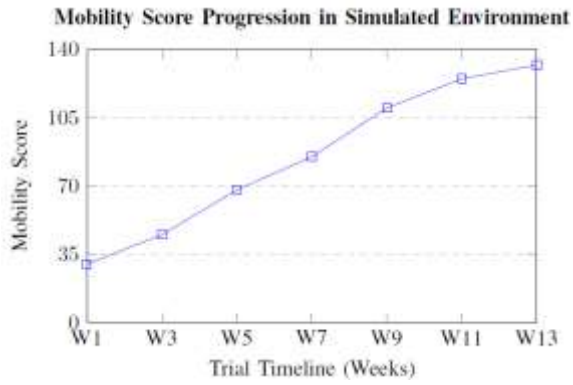

Fig. 4. Progression of Mobility Scores recorded during longitudinal system testing.

VII. COST ANALYSIS AND HEALTH ECONOMICS

The Smart Recovery platform mitigates hardware expenditures by leveraging standard, ubiquitous commercial webcams. By utilizing the TensorFlow.js library to execute the MoveNet 'Thunder' CNN directly within the client's web browser, the system employs an edge-computing paradigm. This offloads the intensive floating-point operations associated with pose estimation from centralized cloud servers to the user's localized GPU via WebGL, effectively reducing the incremental hardware cost to zero.

VIII. LIMITATIONS

While highly capable, the platform possesses inherent technical and environmental limitations. Because the architecture relies heavily on client-side edge computing, tracking performance is fundamentally constrained by the user's localized hardware. Furthermore, 2D webcam-based pose estimation is highly susceptible to environmental variables. Suboptimal ambient lighting or heavy background clutter can degrade tracking accuracy. Biomechanically, 2D optical sensors fundamentally lack true spatial depth perception compared to multi-camera infrared marker systems. Finally, therapeutic efficacy requires further validation through peer-reviewed Randomized Controlled Trials (RCTs) involving clinical populations.

IX. CONCLUSION

The Smart Recovery platform successfully navigates the intersection of deep learning, physical medicine, and software engineering. By leveraging optimized client-side CNNs, the system democratizes access to high-fidelity, markerless motion tracking. Prototype testing demonstrated the capacity to track an average of 412 ± 45 targeted kinematic repetitions per session without performance degradation.

A. Future Scope

Advanced Predictive AI – The integration of Long Short-Term Memory (LSTM) networks will allow the system to analyze historical trajectory data to predict user fatigue plateaus and dynamically adjust game parameters in real-time.

Wearable Sensor Fusion – Future iterations will utilize the Web Bluetooth API to integrate wearable devices, such as smartwatches and EMG bands. This fusion of physiological metrics with optical kinematics will provide a multidimensional view of neuromuscular recovery.

Accessibility and Gamification – To support patients with compounding neurological deficits, the roadmap includes haptic feedback integration and dedicated low-stimulation UI modes with text-to-speech support to minimize cognitive load.

Clinical Trial Commencement – Following the successful technical validation and medical protocol design conducted under the continuous supervision of the clinical co-authors, the project is currently entering the clinical testing phase. This involves deploying the platform in controlled environments with stroke survivors to evaluate longitudinal therapeutic efficacy and real-world recovery outcomes.

REFERENCES

[1] T. E. Twitchell, “The restoration of motor function following hemiplegia in man,” *Brain*, vol. 74, no. 4, pp. 443–480, 1951.

[2] A. R. Fugl-Meyer *et al.*, “The post-stroke hemiplegic patient. 1. a method for evaluation of physical performance,” *Scand. J. Rehabil. Med.*, vol. 7, no. 1, pp. 13–31, 1975.

[3] R. Nakamura and S. Moriyama, “Recovery of impaired motor function of the upper limb after stroke,” *Semanticscholar*, 1992.

[4] H. Feys *et al.*, “Predicting motor recovery of the upper limb after a stroke,” *Semanticscholar*, 2000.

[5] J. Bernhardt *et al.*, “Inactive and alone: physical activity within the first 14 days of acute stroke unit care,” *Stroke*, vol. 35, no. 4, pp. 1005–1009, 2004.

[6] T. J. Kimberley *et al.*, “Comparison of amounts and types of practice during rehabilitation for traumatic brain injury and stroke,” *J. Rehabil. Res. Dev.*, vol. 47, no. 9, pp. 851–862, 2010.

[7] L. Dodakian *et al.*, “A Home-Based Telerehabilitation Program for Patients With Stroke,” *Neurorehabil. Neural Repair*, vol. 31, no. 10-11, pp. 923–933, 2017.

[8] S. C. Cramer *et al.*, “Efficacy of home-based telerehabilitation vs in- clinic therapy for adults after stroke: a randomized clinical trial,” *JAMA Neurol.*, vol. 76, no. 9, pp. 1079–1087, 2019.

[9] G. Fluet *et al.*, “Virtual Rehabilitation of the Paretic Hand and Arm in Persons With Stroke: Translation From Laboratory to Rehabilitation Centers and the Patient’s Home,” *Front. Neurol.*, vol. 12, p. 623261, 2021.

[10] J. Tosto-Mancuso *et al.*, “Gamified neurorehabilitation strategies for post-stroke motor recovery: challenges and advantages,” *Curr. Neurol. Neurosci. Rep.*, vol. 22, no. 3, pp. 183–195, 2022.

[11] S. F. M. Toh *et al.*, “Effectiveness of home-based upper limb rehabilita- tion in stroke survivors: A systematic review and meta-analysis,” *Front. Neurol.*, vol. 13, p. 964196, 2022.

[12] L. Guo *et al.*, “Clinical Study of a Wearable Remote Rehabilitation Training System for Patients With Stroke: Randomized Controlled Pilot Trial,” *JMIR Mhealth Uhealth*, vol. 11, p. e40416, 2023.

[13] D. Edwards *et al.*, “Telerehabilitation Initiated Early in Post-Stroke Recovery: A Feasibility Study,” *Neurorehabil. Neural Repair*, vol. 37, no. 2-3, pp. 131–141, 2023.

[14] S. Facciorusso *et al.*, “Sensor-Based Rehabilitation in Neurological Diseases: A Bibliometric Analysis of Research Trends,” *Brain Sci.*, vol. 13, no. 5, p. 724, 2023.

[15] C. A. J. L. J. Visser *et al.*, "Virtual reality in neuro-rehabilitation: Current developments and future perspectives," *J. Neuroeng. Rehabil.*, 2021.
[16] S. Deterding *et al.*, "From game design elements to gamefulness: defining gamification," in *CHI Conference*, 2011.
[17] A. L. Faria *et al.*, "A survey on the use of motion tracking systems in rehabilitation," *Journal of Biomechanics*, 2014.
[18] K. L. Lee *et al.*, "Effects of exergaming for physical rehabilitation: A systematic review," *Am. J. Phys. Med. Rehabil.*, 2019.
[19] J. Ribeiro *et al.*, "Adaptive algorithms for neuro-rehabilitation: A frame- work for personalized healthcare," *IEEE Trans. Biomed. Eng.*, 2018.